

# Technical Characteristics and Accuracy Capabilities of Delta Differential One-Way Ranging (ADOR) as a Spacecraft Navigation Tool

James S. Border and John A. Koukos  
Jet Propulsion Laboratory  
California Institute of Technology  
Pasadena, California

## Abstract

The technique of determining spacecraft angular position by Delta Differential One-Way Ranging (ADOR) is described. The dependence of measurement accuracy on parameters which define the spacecraft signal spectrum is shown. To enable a ADOR measurement, a spacecraft must emit several tones. A narrow tone spacing is required for integer cycle phase ambiguity resolution, while a wider tone spacing is required for high measurement accuracy. An illustration of ADOR measurement accuracy, using the Mars Observer spacecraft, is presented. Guidelines for specifying spacecraft tone spectra are presented based on typical accuracy and ambiguity resolution needs, on frequency allocation for deep space tracking, on the efficient use of spacecraft signal power, and on the efficient use of ground tracking resources.

## 1. introduction

Very Long Baseline Interferometry (VLBI) is a technique that allows determination of angular position for distant radio sources by measuring the geometric time delay between received radio signals at two geographically separated stations. The observed time delay is a function of the known baseline vector joining the two radio antennas and the direction to the radio source.

An application of VLBI is spacecraft navigation in deep space missions where the measurements at two stations of the phases of tones emitted from a spacecraft are differenced and compared against similarly differenced phase measurements of angularly nearby quasar radio signals. This application of VLBI is known as Delta Differential One-Way Ranging (ADOR).

As such, this technique may necessitate intra-agency cooperation because stations from different agencies can be used as ADOR data collectors for deep space navigation purposes. The NASA Deep Space Network (DSN) has used this technique operationally in a number of missions including Voyager, Magellan, and Vega. Currently, JPL navigation teams are employing ADOR in the Mars Observer and Galileo missions.

This technical position paper intends to provide implementation and performance details of the ADOR technique in order to support forging CCSDS<sup>1</sup> standards for spacecraft VLBI, given the increasing popularity of this method among space agency navigators.

## 2. ADOR and Quasars

An interferometer processes signals recorded at two stations that are geographically separated. The vector  $\vec{B}$  from the first to the second station antenna is called the baseline

<sup>1</sup>Consultative Committee for Space Data Systems

Vector. If the direction  $\hat{s}$  of an extraterrestrial radio source forms an angle  $\theta$  with the baseline vector, then a single radio frequency (RF) source signal wavefront arrives at the two ends of the baseline with a time difference given approximately by

$$\tau_g = -\frac{1}{c}(\vec{B} \cdot \hat{s}) = -\frac{B}{c} \cos \theta \quad (1)$$

assuming that  $B = |\vec{B}|$ . This geometric time delay is an observable quantity with a maximum possible value equal to earth radius/c, or 0.021 sec, and a rate of change due to earth rotation up to 3.0  $\mu\text{sec/sec}$ .

The advantage of very long baselines can be shown by differentiating the above equation with respect to geometric delay:

$$\frac{\partial \theta}{\partial \tau_g} = -\frac{c}{B \sin \theta} \quad (2)$$

in the above equation the longer the baseline  $B$ , the smaller the angular position error for a given error in observed time delay. DSN baseline lengths are between 8,000 and 10,000 km, which yield angular position errors of about 30 nanoradians provided that measurement error in observed time delay is not larger than 1 nanosecond. Note that 30 nrad corresponds to about 22 km plane-of-sky position accuracy at a distance equal to that of Jupiter from the sun.

A ADOR measurement is generated from one-way range measurements made between a spacecraft and each of two ground antennas, and an interferometric time delay measurement of a natural radio source made using the same two antennas.

For a spacecraft, one-way range is determined locally at each station by extracting the phases of two or more tones emitted by the spacecraft. One-way range measurements contain unknown biases due to spacecraft clock offset, receiver clock offset, and ground station instrumental delay. Differential one-way range (DOR) measurements are formed by subtracting the one-way range measurements generated at two stations. The station differencing eliminates the effect of the spacecraft clock offset, but DOR measurements are biased by ground station clock offsets and instrumental delays. The observed quantity in a DOR measurement is analogous to the interferometric delay which may be measured for a broadband radio source, as in Eq. (1).

To generate a ADOR measurement, an interferometric delay measurement of a nongalactic radio source (quasar) is subtracted from a spacecraft DOR measurement. Each station is configured to acquire data from the quasar in frequency channels centered on the spacecraft tone frequencies. This receiver configuration choice ensures that the spacecraft-quasar differencing eliminates the effects of ground station clock offsets and instrumental delays. In fact more is accomplished. By selecting a quasar which is close in an angular sense to the spacecraft, and by observing the quasar at nearly the same time as the spacecraft, the effects of errors in the modeled station locations, earth orientation, and transmission media delays are diminished. A ADOR measurement determines the angular position of a spacecraft in the inertial reference frame defined by the quasars.

The spacecraft and quasar observables are derived from processing digital samples of the radio signals received at each station. The spacecraft tone phases may be extracted using either open-loop or closed-loop techniques, but the quasar radio signal must be recorded

Open-loop. The quasar data samples from two stations must be transmitted to a central processing facility for delay measurement extraction. The DSN stations currently generate open loop recordings of both quasar and spacecraft signals, though an experimental closed-loop tone tracker is now being used during spacecraft observations for real time validation. The same instrumental receiver chain, to the point of signal digitization, must be used for both spacecraft and quasar data acquisition.

The RF signals are selectively downconverted and filtered to generate several baseband channels. Normally, one baseband channel is centered on each spacecraft tone. The instantaneous channel bandwidth is typically in the range of a few hundred kilohertz to a few Megahertz. The DSN operational system, referred to as the Narrow Channel Bandwidth (NCB) VLB System [Liewer 1988], uses a 250 kHz channel bandwidth. The analog signal in each channel is digitally sampled at the Nyquist rate, and then either recorded or input to the tone tracker. For DSN data acquisition, data samples are transmitted to the Network Operations Control Center at JPL for observable extraction.

For spacecraft data processing, an *a priori*  $i$  tone phase model is computed, based on the nominal measurement geometry and transmitter frequency. A search in frequency is conducted to locate the actual tone frequency, and then tone phase is extracted using a phase-locked loop. This procedure is repeated for each tone at each station. Denote the station-differenced received phase, for a spacecraft tone with transmitter frequency  $\omega_i$ , by  $\phi_s(\omega_i)$ . Then the spacecraft delay observable is given by

$$\tau_g^{s/c} = \frac{\phi_s(\omega_2) - \phi_s(\omega_1)}{\omega_2 - \omega_1}. \quad (3)$$

The frequency separation between the two outermost DOR tones is referred to as the spanned bandwidth of the spacecraft signal.

For quasar data processing, the data samples in each baseband channel from two stations are cross-correlated to produce an estimate of interferometric phase  $\phi_Q(\bar{\omega}_i)$  at the channel centroid frequency  $\bar{\omega}_i$  [Thomas 1987]. Interferometric phase for a broadband radio source is analogous to station-differenced phase for a sinusoidal radio source. The quasar delay observable is given by

$$\tau_g^{QSR} = \frac{\phi_Q(\bar{\omega}_2) - \phi_Q(\bar{\omega}_1)}{\bar{\omega}_2 - \bar{\omega}_1}. \quad (4)$$

The centroid of the receiver bandpass for channel  $i$  takes the role of the discrete frequency of DOR tone  $i$ .

### **3. Spacecraft DOR Tone Structure**

A spacecraft transponder must emit several tones (referred to as DOR tones) spanning some bandwidth to enable a DOR measurement. The DOR tones are generated by modulating a pure sine wave, or pure square wave onto the downlink carrier at either S-band, X-band, or Ka-band. Requirements on the number of DOR tones, tone frequencies, and tone power are based on the expected *a priori* knowledge of spacecraft angular position and on the required differential range measurement accuracy, as discussed below. Generally, a narrow spanned bandwidth is needed for integer cycle ambiguity resolution based on  $\alpha$

*priori* knowledge of spacecraft angular position, while a wide spanned bandwidth is needed for high measurement accuracy.

'1'Ones generated by modulating a carrier signal by a single square wave provide a low performance option. The ratio of maximum spanned bandwidth to minimum spanned bandwidth, for tones above the detection threshold, is usually in the range of 1 to 6. To provide higher performance (i.e. a wider spanned bandwidth with more power in the outer tones), while still providing a spanned bandwidth narrow enough for integer cycle ambiguity resolution, more DOR tones are needed. Sine waves are normally used in multi-tone systems based on efficiency considerations.

For example, ADOR measurements were made for the Voyager spacecraft using high order harmonics of the 360 kHz telemetry square wave subcarrier signal. More accurate ADOR measurements have been made of the Mars Observer spacecraft using two sine wave signals (3.825 MHz and 19.125 MHz) modulated onto the downlink carrier.

It is preferable for DOR tones to be frequency coherent with the downlink carrier. This facilitates the detection of weak DOR tones by allowing the use of a phase model derived from the received carrier signal. Also, the transmitted spanned bandwidth of the DOR tones, which must be known for the generation of a differential range observable from received phase measurements, will in this case be a defined multiple of the transmitted carrier frequency.

The most usual DOR tone modulation formats are presented next.

### **3.1 DOR Tones Generated from Modulation by Two Sinewaves**

Two sinusoidal tones with circular frequencies  $\omega_1$  and  $\omega_2$  are phase modulated on the downlink carrier signal with peak modulation indices  $m_1$  and  $m_2$ , respectively:

$$s(t) = \sqrt{2P_T} \cos(\omega_c t + m_1 \sin(\omega_1 t) + m_2 \sin(\omega_2 t)). \quad (5)$$

The above expression may be expanded to separate the carrier and main DOR tone components of the signal from higher order harmonics:

$$s(t) = \sqrt{2P_T} [ J_0(m_1)J_0(m_2)\cos(\omega_c t) - 2J_1(m_1)J_0(m_2)\sin(\omega_c t)\sin(\omega_1 t) - 2J_0(m_1)J_1(m_2)\sin(\omega_c t)\sin(\omega_2 t) + \text{higher harmonics} ] \quad (6)$$

where  $J_0$  and  $J_1$  are Bessel functions of the first kind. The modulation produces tones at frequencies of  $\omega_c \pm \omega_1$  and  $\omega_c \pm \omega_2$ . Modulation indices may be chosen to put more power in the outer tones, while putting just enough power in the inner tones to provide for ambiguity resolution.

The powers allocated to the carrier and the tones are easily deduced from the above expression:

$$\begin{aligned} P_c &= P_T J_0^2(m_1)J_0^2(m_2), \\ P_1 &= P_T J_1^2(m_1)J_0^2(m_2), \text{ and} \\ P_2 &= P_T J_0^2(m_1)J_1^2(m_2). \end{aligned} \quad (7)$$

The corresponding modulation losses are expressed as the fractions below:

$$\begin{aligned}
\frac{P_c}{P_T} &= J_0^2(m_1)J_0^2(m_2), \\
\frac{P_1}{P_T} &= J_1^2(m_1)J_0^2(m_2), \text{ and} \\
\frac{P_2}{P_T} &= J_0^2(m_1)J_1^2(m_2).
\end{aligned} \tag{8}$$

The above two-sinewave signaling scheme is used on Mars Observer. For Mars Observer the nominal values Of the DOR modulation indices are  $m_1=0.64$  rad and  $m_2=0.32$  rad for the  $f_1=19.125$  MHz and  $f_2=3.825$  MHz DOR tones, respectively. Such values yield modulation losses PC/PIU-1,14 dB,  $P_1/P_T=-10.57$  dB, and  $P_2/P_T=-16.94$  dB.

### 3.2 DOR Tones Generated from Modulation by One Squarewave

In this case, one squarewave signal with unit amplitude and frequency  $\omega_1$  is phase modulated on the downlink carrier to generate a downlink signal with multiple tones:

$$s(t) = \sqrt{2}P_T \cos(\omega_c t + m_1 \text{sqwv}(\omega_1 t)). \tag{9}$$

The cosine of the sum may be expanded to give:

$$s(t) = \sqrt{2}P_T \cos(m_1 \text{sqwv}(\omega_1 t)) \cos(\omega_c t) - \sqrt{2}P_T \sin(m_1 \text{sqwv}(\omega_1 t)) \sin(\omega_c t). \tag{10}$$

The second term On the right hand side is a carrier signal multiplied by a square wave with amplitude  $\sin(m_1)$ . This square wave has a Fourier expansion

$$\sin(m_1 \text{sqwv}(\omega_1 t)) = \sin(m_1) \frac{4}{\pi} \sum_{k=1}^{\infty} \frac{\cos[(2k-1)\omega_1 t]}{2k-1}, \tag{11}$$

and Eq. (10) may be rewritten as

$$\begin{aligned}
s(t) &= \sqrt{2}P_T \cos(m_1 \text{sqwv}(\omega_1 t)) \cos(\omega_c t) - \\
&\quad \sqrt{2}P_T \sin(m_1) \frac{4}{\pi} \sum_{k=1}^{\infty} \frac{\cos[(2k-1)\omega_1 t]}{2k-1} \sin(\omega_c t).
\end{aligned} \tag{12}$$

The second term On the right hand side produces tones at odd multiples Of the subcarrier frequency spaced about the carrier. The modulation loss formula for the squarewave harmonics is easily calculated from the coefficients Of the above expression:

$$\frac{P_k}{P_T} = \frac{4}{\pi} \frac{1}{(2k-1)^2} \sin^2(m_1) \text{ at } \omega_c \pm (2k-1)\omega_1 \text{ for } k = 1, 2, 3, \dots \tag{13}$$

Considering that the cosine is an even function, the first term On the right hand side Of Eq. (10) would appear to produce a pure carrier signal with  $1/1' = -\cos^2(m_1)$ . **However**, since the square wave must be band limited, the function  $\cos(m_1 \text{sqwv}(\omega_1 t))$  is actually a spike train with period  $2\pi/(2\omega_1)$  and amplitude  $(1 - \cos m_1)$ . This spike train produces even harmonics of the square wave frequency about the carrier signs 1 [1 Hildebrand and Yunc 1982]. For high rate subcarriers, say above 360 kHz, the sc. tones may be detectable and

usable as DOR tones. The power in the even harmonics is proportional to  $(1 - \cos m_f)^2$ , but the actual power depends on the shape of the subcarrier signal. The total power in the even harmonics, excluding the carrier signal itself, is usually quite small.

When telemetry modulation is imposed on the subcarrier, the odd harmonics are spread and are not usable for DOR measurements. The even harmonics generated from the spike train, on the other hand, remain as pure tones. High order even harmonics of the high rate telemetry subcarrier, at a level of about -30 dB relative to the total signal power, were used as DOR tones for the Voyager and Magellan spacecraft. While such measurements of opportunity may be useful, it is difficult to plan for this case since the spectrum depends on the precise shape of the subcarrier signal.

Normally, low order odd harmonics of the square wave modulation would serve as DOR tones. This scheme was used on the Vega and Phobos missions.

As an example consider a fully suppressed carrier ( $m_f = 90^\circ$ ). Then the suppression of the first two odd square wave harmonics is given by:

$$\begin{aligned}\frac{P_1}{P_T} &= -3.92 \text{ dB and} \\ \frac{P_2}{P_T} &= -13.46 \text{ dB}\end{aligned}\tag{14}$$

#### 4. Signal Detection Requirements

Signal detection requirements are stated in terms of the voltage signal-to-noise ratio for an 1-sec average. For a sinusoidal spacecraft signal, the requirement may be expressed in terms of tone power to noise power spectral density. For a broadband quasar signal, the requirement may be expressed in terms of source flux, antenna gain, antenna noise temperature, and recorded bandwidth. The requirements given here are not theoretical limits, but rather practical thresholds based on typical system coherence times\* and operational data processing methods.

The requirements are:

$$\text{SNR}_{V1}^{S/C} \geq 5.0 \quad \text{for a spacecraft tone, and} \tag{A}$$

$$\text{SNR}_{V1}^{QSR} \geq 1.3 \quad \text{for a broadband quasar source,} \tag{B}$$

where  $\text{SNR}_{V1}$  is the voltage signal-to-noise ratio for an 1-sec average. The difference in detection criteria is due to the effective coherence time. Quasars signal detection is based on an averaging time of about 60 sec, since geometric delay models for quasar signals are quite well known *a priori*. But spacecraft signal detection must usually be based on an averaging time of order 1 sec, since tone phase models are not well known *a priori*. If the spacecraft transmits carrier signal which satisfies criterion (A), and if differential range

\* The system coherence time may be defined as the time for the actual signal phase to wander by 0.1 cycle from the model signal phase.

measurements are to be made using side tones which are coherent multiples of the carrier signal, then the detection requirement for the sidetones may be relaxed to

$$\text{SNR}_{V1}^{S/C} \geq 1.3 \quad \text{for a spacecraft tone which is a coherent multiple of a spacecraft carrier signal which satisfies criterion (A).} \quad (c)$$

For a spacecraft tone, the 1-sec voltage SNR is related to  $P_{\text{tone}}/N_0$ , the tone power to noise power in a 1 Hz bandwidth, by

$$\text{SNR}_{V1}^{S/C} = \sqrt{\frac{2}{\pi}} \sqrt{\frac{2 P_{\text{tone}}}{N_0}} \quad (15)$$

where the factor  $2/\pi$  is due to 1-bit sampling of the signal. The factor  $2/n$  is replaced by unity for a system which supports multi-level sampling. Using Eq. (15), criteria (A) and (C) may be rewritten as

$$\frac{P_{\text{tone}}}{N_0} \geq 13 \text{ dB} \cdot \text{Hz} \quad \text{for a spacecraft tone,} \quad (A')$$

$$\frac{P_{\text{quasar}}}{N_0} \geq 1 \text{ dB} \cdot \text{Hz} \quad \text{for a spacecraft tone which is a coherent multiple of a spacecraft carrier signal which satisfies criterion (A'),} \quad (c')$$

For a broadband quasar signal, the 1-sec voltage SNR is related to system parameters by [Thomas 1981]

$$\text{SNR}_{V1}^{\text{QSR}} = K_L \frac{2}{\pi} \sqrt{\frac{T_{q1} T_{q2}}{T_{s1} T_{s2}}} \sqrt{N_b} \quad (16)$$

where  $K_L$  is the system loss factor (0.8 to 1.0), the factor  $2/\pi$  is due to 1-bit sampling,  $T_{qi}$ ,  $T_{si}$  are the correlated source temperature, and system noise temperature at antenna  $i$ , and  $N_b$  is the number of data samples in 1 second. The correlated source temperature for antenna  $i$  is given approximately by

$$T_{qi} = (0.00030) \epsilon_i \pi r_i^2 S_c \quad (17)$$

where  $\epsilon_i$ ,  $r_i$  are the efficiency and radius (m) for antenna  $i$  and  $S_c$  is the correlated source flux (Jansky or Jy). For the DSN NCB VLBI System operating at X-band,  $K_L = 0.8$ ,  $\epsilon = 0.60$  for a 70-m diameter antenna at  $10^\circ$  elevation,  $\epsilon = 0.68$  for a 34-m diameter antenna at  $10^\circ$  elevation,  $T_s \approx 30$  K, and  $N_b = 500,000$ . Using these nominal values in Eqs (16) and (17), the detection criterion (B) is restated in terms of minimum required correlated source flux for DSN antenna pairs in Table 1.

Table 1. Minimum correlated source flux for signal detection at X-band using the NCB VLBI System.

DSN Antenna Pair	Minimum Correlated Flux
70m-70m	0.16 Jy
70m-34m	<b>0.30</b> Jy
34m-34m	0.60 Jy

## 5. ADOR Measurement Accuracy

The precision of a spacecraft DOR measurement, given by Eq. (19) below, depends on the received tone power to noise power ratio and on the spanned bandwidth of the tones. But the accuracy of a ADOR measurement, given by the sum of Eqs. (19) through (28) below, also depends on the precision of the quasar delay measurement, on knowledge of the quasar position, on clock stability, on instrumental phase response, and on uncertainties in earth platform models and transmission media delays. An error budget for a **ADOR** measurement depends on observation geometry and all of these factors. Specifications for DOR tone power level and spanned bandwidth are based on total ADOR measurement accuracy, rather than only on spacecraft DOR measurement precision. Simplified formulae are given here for evaluating ADOR measurement accuracy to provide a basis for developing transponder specifications.

Normally, a ADOR pass consists of three "scans" of data recording each of a few minutes duration. The observing sequence is spacecraft-quasar-spacecraft. A ADOR observable is generated from the linear combination of the three measurements which eliminates linear temporal errors. The observed quantity in a ADOR observation is time delay.

### 5.1 Spacecraft SNR

The precision of measurement of tone phase, for  $T_L$  sec of data, is described by the error in the tone phase measurement:

$$\epsilon_\varphi = \frac{1}{2\pi\sqrt{T_L} \cdot \text{SNR}_{V1}^{S/C}} \text{ Cycles.} \quad (18)$$

A DOR measurement is formed from tone phase measurements, received at two stations, as in Eq. (3). Assuming that the four tones have the same received power to noise ratio, the delay error  $\epsilon_\tau$  is given by

$$\epsilon_\tau = \frac{2}{2\pi f_{BW} \sqrt{\frac{T_{obs}}{N_c} \text{SNR}_{V1}^{S/C}}} \text{ sec} \quad (19)$$

where  $f_{BW}$  is the spanned bandwidth (Hz),  $T_{obs}$  is the observation scan length (sec), and  $N_c$  is the number of channels of data recorded by time multiplexing. Set  $N_c$  to unity if data channels are recorded in parallel.



## 5.2 Quasar SNR

The quasar delay measurement error is given by [Thems 1981]

$$\epsilon_\tau = \frac{\sqrt{2}}{2\pi f_{BW} \sqrt{\frac{T_{obs}}{N_c} SNR_{V1}^{QSR}}} \text{ sec.} \quad (20)$$

The spanned bandwidth for the quasar measurement must be selected to be the same as for the spacecraft tones to ensure cancellation of the effects of dispersive instrumental phase shifts.

## 5.3 Quasar Position

Uncertainty in the position coordinates of the reference quasar will cause a ADOR delay error through the relation given by Eq. (1). Assuming a spherical position uncertainty of  $\epsilon_\theta$  rad, the delay error is

$$\epsilon_\tau = \frac{B_p}{c} \epsilon_\theta \text{ sec} \quad (21)$$

where  $B_p$  is the projected baseline length.

## 5.4 Clock Instability

Instability in the station frequency standard Or temporal instabilities in instrumental com Orients cause a delay error which depends On the. time separation between the spacecraft and quasar observations. The delay error is given by

$$\epsilon_\tau = \sqrt{2} T_{S/C-QSR} \epsilon_{Aff} \text{ sec} \quad (22)$$

where  $T_{S/C-QSR}$  (sec) is the time separation between the spacecraft and quasar observations and  $\epsilon_{Aff}$  is the composite Allan standard deviation of the station frequency standard and frequency distribution system.

## 5.5 Instrumental Phase Ripple

A quasar signal is affected by the station instrumental phase response across the bandpass, whereas a spacecraft tone is affected by the instrumental phase shift at the tone frequency. A deviation of the phase response from a smooth phase versus frequency transfer function is referred to as phase ripple. Instrumental phase ripple of  $\epsilon_\phi$  deg causes a delay error of

$$\epsilon_\tau = \sqrt{2} \sqrt{2} - \frac{1}{f_{BW}} \frac{\epsilon_\phi}{360} \text{ sec} \quad (23)$$

assuming the phase ripple is independent in each channel and at each station, and assuming that the phase ripple averages to zero for the quasar measurement.

### 5.6 Station Location

Uncertainty in station coordinates causes a delay error which depends on the spacecraft-quasar angular separation. Assuming a spherical uncertainty  $\epsilon_{stn}$  in baseline position components, the delay error is

$$\epsilon_{\tau} = A\theta \frac{\epsilon_{stn}}{c} \text{ sec} \quad (24)$$

where  $A\theta$  is the spacecraft-quasar angular separation (rad).

### 5.7 Earth Orientation

Uncertainty in the orientation of the Earth in inertial space causes a delay error of the same form as station location uncertainty. The delay error is

$$\epsilon_{\tau} = A\theta \frac{\epsilon_{UTPM}}{c} \text{ sec} \quad (25)$$

where  $\epsilon_{UTPM}$  is the positional uncertainty in UT1-UTC and polar motion at the Earth's surface.

### 5.8 Troposphere

Uncertainty in the zenith tropospheric delay, primarily due to variations in the wet component, causes a systematic delay error of

$$\epsilon_{\tau} = \frac{\rho_z}{c} \left| \frac{1}{\sin \gamma_{SC}} - \frac{1}{\sin \gamma_{QSR}} \right| \text{ sec} \quad (26)$$

where  $\rho_z$  is the zenith uncertainty,  $\gamma_{SC}$  is the spacecraft elevation angle, and  $\gamma_{QSR}$  is the quasar elevation angle. There is a term of this form for each station.

### 5.9 Ionosphere

The ionospheric error depends on signal frequency and path delay uncertainty after calibration. A rough empirical formula, based on comparisons of ionospheric calibrations derived from Faraday rotation measurements with dual frequency quasar VLBI measurements [Edwards 1991], is given by

$$\epsilon_{\tau} = \frac{(1.46 + 16.9 A\theta)}{f_{RF}^2} \times 10^{-9} \text{ sec} \quad (27)$$

where  $\Delta\theta$  is the spacecraft-quasar angular separation (rad) and  $f_{RF}$  is the signal radio frequency (GHz).

### **5.10 Solar Plasma**

The solar plasma error depends on signal frequency and proximity of the the signal raypaths to the sun. An estimate for the delay error is given by [Callahan 1978]

$$\epsilon_{\tau} = \frac{0.013}{f_{RF}^2} [\sin(SEP)]^{1.3} \left( \frac{B_p}{v_{sw}} \right)^{0.75} \times 10^{-9} \text{ sec} \quad (28)$$

where  $SEP$  is the sun-radio source angular separation,  $B_p$  is the projected baseline length (km) at the point of signal closest approach to the sun,  $v_{sw}$  (km/sec) is the solar wind velocity, and  $f_{RF}$  is the signal frequency (GHz). '1' here is a term of this form for both the spacecraft and the quasar,

### **5.11 Root-Sum-Square**

The predicted ADOR measurement accuracy is computed as the RSS of the above ten terms. Equation (2) may be used to relate delay measurement accuracy to angular position accuracy.

## **6. Mars Observer ADOR Error Budget**

The formulae of Section 5 show how ADOR measurement accuracy depends on spacecraft transponder parameters, on observation geometry and scan length, on instrumental stability, and on the accuracy of external calibrations. Nominal values for these parameters, applicable for the cruise phase of the Mars Observer mission and for data acquisition using the DSNNCBVLBI System, are given in Table 2. Figure 1 shows the error budget which corresponds to these parameter values.

Table 2. Nominal parameter values for evaluation of Mars Observer AIDOR error budget.

Term	Description	Nominal Value
$P_{tone}/N_0$	IDOR tone power to noise power spectral density	25 dB•Hz
$K_i$	System loss factor (quasar data acquisition)	0.8
$N_b$	Number of quasar data samples per second	500,000
$T_{si}$	System noise temperature, antenna i	Antenna 1: 30 K Antenna 2: 30 K
$\epsilon_i$	Efficiency, antenna i	Antenna 1: 0.60 Antenna 2: 0.68
$r_i$	Radius, antenna i	Antenna 1: 35 m Antenna 2: 17 m
$S_c$	Correlated source flux	0.8 Jy
$f_{BW}$	Spanned bandwidth	38.25 MHz
$T_{obs}$	Observation scan length	S/C: 10 min QSR: 14 min
$N_c$	Number of time-multiplexed frequency channels	4
$\epsilon_\theta$	Quasar position uncertainty	5 mrad
$B_p$	Projected baseline length	8000 km
$T_{S/C-QSR}$	Time separation between S/C and QSR observation	12.5 min
$\epsilon_{NIJ}$	Clock Instability	10 <sup>-14</sup>
$\epsilon_\phi$	Instrumental phase ripple	0.5 deg
$\Delta\theta$	Spacecraft-quasar angular separation	10 deg
$\epsilon_{sm}$	Baseline coordinate uncertainty, each component	3 cm
$\epsilon_{UTM}$	Baseline orientation uncertainty, each component	5 cm <sup>†</sup>
$\rho_z$	Zenith troposphere delay uncertainty, each station	4 cm
$\gamma_{S/C}$	Spacecraft elevation angle	Antenna 1: 20 deg Antenna 2: 25 deg
$\gamma_{QSR}$	Quasar elevation angle	Antenna 1: 25 deg Antenna 2: 20 deg
$f_{RF}$	Signal radio frequency	8.4 GHz
$SEP$	Sun-Earth-Source angle	50 deg
..	Excluded variables	400 hours

<sup>†</sup> Realtime prediction uncertainty for UJ1-UJ1C is 30 cm. A processing delay of 1 week is necessary to obtain 5 cm accuracy for earth orientation calibrations.

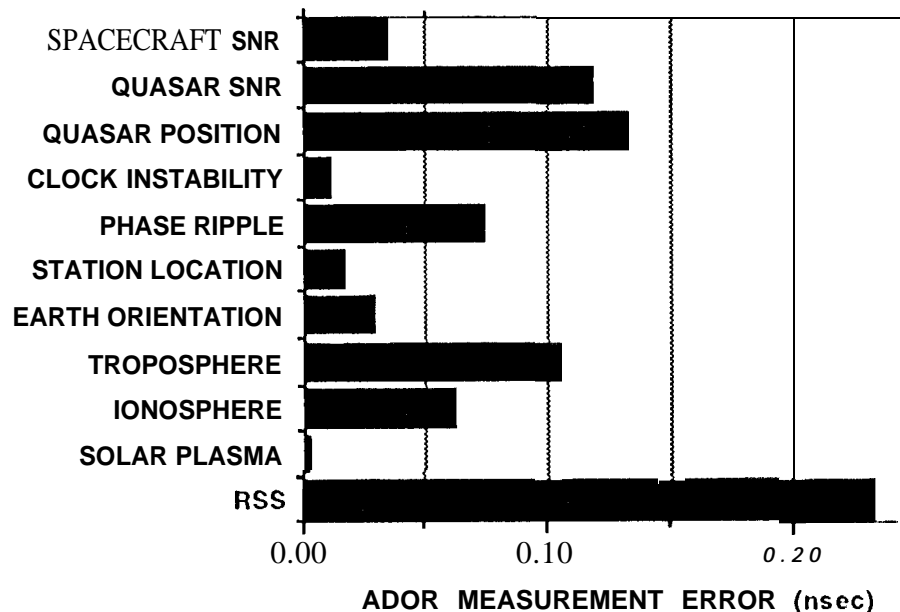


Figure 1. ADOR error budget ( $1-\sigma$ ) for Mars Observer, based on the nominal parameter values given in Table 2.

The RSS ADOR measurement accuracy of 0.23 nsec, shown in Fig. 1, provides an angular position accuracy of 9 nrad for a projected baseline length of 8000 km. The dominant errors due to quasar SNR, quasar position, instrumental phase ripple, troposphere, and ionosphere vary considerably with observing schedule and geometry, so that actual performance for Mars Observer ADOR accuracy falls within a range of values from 0.1 nsec to 0.7 nsec. The DOR tones emitted by the Mars Observer transmitter clearly enable ADOR measurement accuracy, using the DSN, of better than 1 nsec.

Perhaps the single most important parameter in the error budget is the spanned bandwidth of the spacecraft DOR tones. Doubling this bandwidth, while holding other parameters fixed, will halve the errors due to spacecraft SNR, quasar SNR, and instrumental phase ripple. Once antennas and data acquisition terminals are implemented, little control is available over the other parameters which affect quasar SNR and instrumental phase ripple. For example, the quasar scan length must be increased by a factor of four to halve the error due to quasar SNR if other parameters are held fixed.

## 7. Integer Cycle Phase Ambiguity Resolution

Only the fractional part of signal phase can be measured; the integer part must be determined from *a priori* knowledge. This phase ambiguity leads to a ADOR time delay ambiguity equal to the reciprocal of the minimum spanned bandwidth. For ambiguity resolution at the 99% confidence level, the spacecraft geometric delay must be known *a priori* in the radio reference frame to 1/6 of the reciprocal minimum spanned bandwidth.

Delay ambiguities in observables generated from wider spanned bandwidths are resolved successively by using delay estimates from the narrower spanned bandwidths.

For example, the angular position of the spacecraft must be known *a priori* with a 1- $\sigma$  accuracy of 1  $\mu$ rad to confidently resolve the ambiguity in a  $\Delta$ DOR measurement which was made by using a 5 MHz spanned bandwidth and a 10,000 km projected baseline length. This level of accuracy is normally achieved using a few passes of Doppler and range data.

Once the delay ambiguity has been resolved for a spanned bandwidth of  $f_{BW1}$ , then the ambiguity may be resolved for a spanned bandwidth of  $\eta f_{BW1}$ , provided that

$$\eta \leq 1/(6\sigma_{\phi_1}), \quad (29)$$

where  $\sigma_{\phi_1}$  is an upper bound on the 1- $\sigma$  dispersive error (cycles) in the channel-differenced, station-differenced phase measurement used to generate delay at the spanned bandwidth  $f_{BW1}$ . Dispersive errors, caused by system thermal noise, instrumental phase ripple, and interchannel oscillator phase drift, are conservatively bounded by 0.03 cycle, indicating that spanned bandwidth may reliably increase by a factor of 5.5.

In a multi-tone system, a tone frequency ratio of  $f_2/f_1 = 12$  is consistent with a jump of at most 5.5 in spanned bandwidth. The ambiguity is first resolved using the carrier tone and one DOR tone at frequency separation  $f_1$  from the carrier. Next, the ambiguity at spanned bandwidth  $2f_1$  is resolved. The resulting delay estimate is used to resolve the ambiguity at spanned bandwidth  $f_2 - f_1$ , which may finally be used to resolve the ambiguity at spanned bandwidth  $2f_2$ . Note that  $f_2/f_1 = 12$  follows from  $(f_2 - f_1)/(2f_1) = 5.5$ .

Dispersive phase measurement errors may be considerably less than 0.03 cycle for a highly linear ground receiver system operating with strong signal levels. For this case use Eq. (29) to determine the greatest allowable jump in spanned bandwidth.

## **8 Proposed Spacecraft DOR '1011' Spectra**

The material developed in Sections 1 through 8 may be used to derive specifications for the number of spacecraft DOR tones, tone powers, and tone frequencies, given mission navigation accuracy requirements. Guidelines for DOR tone spectra are presented here, based on typical accuracy and ambiguity resolution needs, on frequency allocation for deep space tracking, on the efficient use of spacecraft signal power, and on the efficient use of ground tracking resources. The case of a single spacecraft in interplanetary cruise is considered first. Next, the special case of differential VLBI measurements made between two spacecraft is considered.

### **8.1 Cruise Navigation Support: Ambiguity Resolution and Measurement Accuracy**

A minimum spanned bandwidth of 5 MHz or less is recommended so that integer cycle delay ambiguities may be resolved, for the longest baselines, using only 1  $\mu$ rad *a priori* knowledge of spacecraft angular position. This spanned bandwidth may be realized using the carrier signal and the first harmonic of a DOR tone whose frequency is 5 MHz or less. The required *a priori* knowledge may be obtained by using Doppler or range data, or by using the unambiguous AVI BL delay rate observables which can always be generated from

the phase measurements used to generate a ADOR observable, or by making a ADOR measurement using the spacecraft telemetry signal. For some cases the *a priori* trajectory knowledge may be much better than 1  $\mu$ rad, and the minimum spanned bandwidth may be much greater than 5 MHz.

The final ADOR measurement is derived using the widest spanned bandwidth provided by the DOR tones. Measurement accuracy, as a function of spanned bandwidth, is plotted in Fig. 2. The separate errors due to spacecraft SNR, quasar SNR, and instrumental phase ripple are shown; the RSS of all other measurement system errors is shown with label "other errors"; the total RSS error is shown. This error computation assumes that data are acquired at X-band using a DSN 70m-34m antenna pair with the NCB VLBI System, the quasar flux is 0.5 Jy, and the received spacecraft DOR tone power to noise spectral density is 15 dB·Hz. All other assumptions are as given in Table 2.

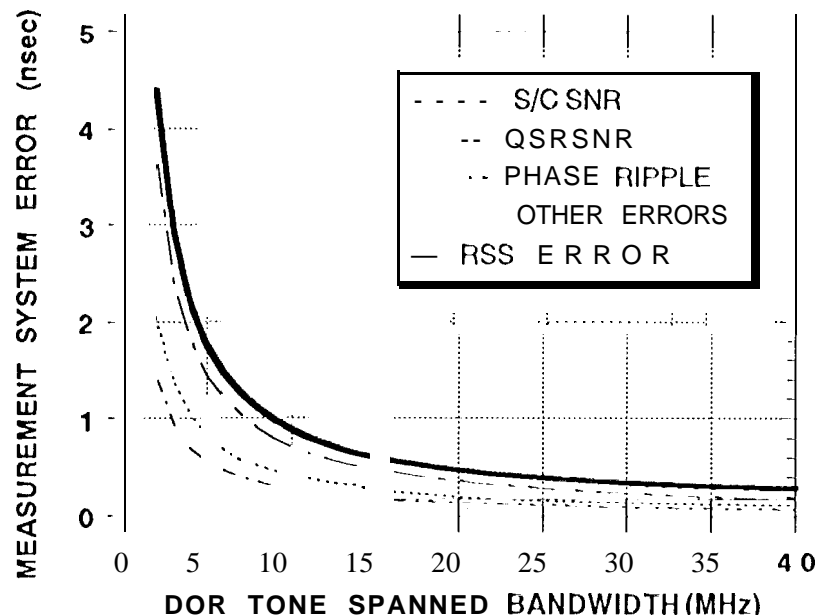


Figure 2. Typical ADOR measurement system errors at X-band as a function of spacecraft tone spanned bandwidth.

As seen from Fig. 2, a spanned bandwidth of 35 MHz or greater is needed to reduce the errors which depend on spanned bandwidth to a level comparable with typical values for other measurement system errors. Measurements generated using a more narrow spanned bandwidth do not make efficient use of DSN resources, since more station time is required to obtain the same level of trajectory accuracy. For this same reason, it is recommended that the received power to noise spectral density ratio be at least 15 dB·Hz for the outer most DOR tones. If the signal level is much less than 15 dB·Hz, then the spacecraft scan length must be much longer than the quasar scan length to reduce the error due to spacecraft SNR to a level comparable with the error due to quasar SNR. The inner DOR tones, which are only used for ambiguity resolution, need only be strong enough to detect.

The frequency bandwidth allocation for deep space tracking is 10 MHz at S-band (2.3 GHz), 50 MHz at X-band (8.4 GHz), and 400 MHz at Ka-band (32 GHz). The recommendations, which are consistent with these allocations, are given in Table 3.

Table 3. Proposed spacecraft DOR tone spectra for deep space tracking.

Frequency Band	Proposed DOR Tone Spectra		Accuracy*
	Number of DOR Tones	DOR Tone Frequencies (Approximate)	
S-band	1	4 MHz	41 mrad
X-band	2	4 MHz and 20 MHz	9 mrad
Ka-band	3	4 MHz, 20 MHz, and 120 MHz	7 mrad

\* The assumptions used in this accuracy prediction are as given in Table 2 except: signal frequency is 2.3 GHz for S-band, 8.4 GHz for X-band, 32 GHz for Ka-band; DOR tone power to noise power spectral

temperature is 30 K for S-band and X-band, and 60 K for Ka-band; X-band, and 0.25 Jy for Ka-band; charged particle errors are scaled by converted from nsec to mrad assuming 8000 km baseline projection.

The DOR measurements are generated using the  $\pm 1^{\text{st}}$  harmonics of the DOR tones. At S-band, one tone provides for ambiguity resolution and provides the widest bandwidth that fits within the allocation. At X-band, two tones are generally needed to provide for both ambiguity resolution and for high accuracy. At Ka-band, a wider spanned bandwidth is necessary to reduce the size of the error due to quasar SNR, since, for Ka-band relative to X-band, quasar flux is reduced and system noise temperature is higher. Three tones are needed at Ka-band to provide for successive ambiguity resolution and to produce a sufficiently wide spanned bandwidth.

*The proposed tone frequencies listed in Table 3 are meant to be approximate values, not exact values.* For example, at X-band, one tone in the range of 2 to 5 MHz, and a second tone in the range of 17.5 to 24 MHz, satisfies all the guidelines.

The ADOR measurement accuracy shown in Table 3 is the typical value attained today using the DSN NCB VLBI System for S-band or X-band. The value shown for Ka-band is a projection. It should be noted that a number of sources of error, such as quasar position, quasar SNR, and uncalibrated tropospheric delay, could be significantly reduced in the future. Thus total measurement accuracy could possibly be improved by incorporating a wider spacecraft DOR tone spanned bandwidth or by transmitting more power in the outer DOR tones.

## 8.2 Special Cases: Spacecraft-Spacecraft AVI/BI

When one spacecraft is approaching a planet at which another spacecraft is already in orbit or landed on the surface, then AVI/BI measurements between the two spacecraft can provide target-relative angular position. When two or more spacecraft are operating in orbit or on the surface of the same planet, then earth-based Same-Beam Interferometry (SBI) measurements can increase both the efficiency and the accuracy of positioning. For these applications, to achieve the best performance, there are additional compatibility requirements on the signal spectra of the spacecraft to be jointly observed. The signal requirements depend on the characteristics of the ground receiver system and on the



navigation performance requirements. The relevant issues are introduced here, but detailed design criteria are not given.

**8.2A Spacecraft-Target AVI.BI.** Studies have shown that the use of spacecraft-spacecraft AVI.BI for planetary approach navigation can reduce targeting errors by a factor of two to three relative to solutions based on Doppler, range, and spacecraft-quasar ADOR [Edwards *et al.* 1991]. The ADOR technique employs observations of two radio sources at the same frequency in order to eliminate the effects of dispersive phase shifts in the station receiver chain. To make AVI.BI measurements between two spacecraft, either the two spacecraft must emit DOR tones at or near the same frequencies, or external calibrations must be used to reduce the effects of dispersive instrumental phase shifts. Here, "the same frequency" means that both signals must fall within the same baseband receiver channel, and that each spacecraft must provide the same spanned bandwidth. Instrumental effects are analyzed in [Border *et al.* 1992].

The DSN NCB VI.BI System has 250 kHz baseband channels. Each channel is downconverted from RF using an analog mixing signal. An arbitrary phase shift is introduced in each channel by this process. For spacecraft-spacecraft AVI.BI, where the two spacecraft do not emit compatible signals, the receiver system must be calibrated either by observing a quasar or by injecting a comb of calibration tones locally at each station. These calibration techniques are operations that are cumbersome and degrade the data accuracy.

The spacecraft signal compatibility requirements could be relaxed if the station receiver system digitized the entire passband before downconverting selected portions of the spectrum to baseband. In an all-digital system, the two spacecraft need not transmit at the same frequencies; spacecraft tone phases could be extracted locally in real time, and spacecraft-spacecraft AVI.BI observables could be generated immediately following acquisition.

**8.2B Orbiter-Orbiter SBI.** For two planetary orbiters, SBI data are generated from carrier phase measurements acquired simultaneously at two stations from the two spacecraft. The SBI data sense the relative motion of the spacecraft in the plane of the sky. Studies have shown that SBI data, when combined with Doppler data, can improve orbital accuracy by an order of magnitude relative to solutions generated from only Doppler data [Folkner and Border 1992]. No DOR tones are needed to enable this measurement; each spacecraft must transmit a carrier signal. Data arcs of 1 to 2 hr are needed. A carrier phase bias must be estimated for each arc; ambiguity resolution is not required. The spacecraft signals should be in the same RF band, but there are no further compatibility requirements for this application.

**8.2C Lander-Rover SBI.** The SBI measurement becomes extremely accurate as the angular separation between radio sources decreases. For the case of a rover and lander, accuracy as good as 10  $\mu$ rad is possible. Studies have shown that SBI measurements, combined with line-of-sight range measurements, could enable nearly instantaneous earth-based positioning of a rover relative to a lander at the 1-m level [Kahn *et al.* 1992]. To achieve this level of accuracy, the phase ambiguity must be resolved in the carrier cycle.

It follows from the analysis in Section 7 that carrier cycle ambiguity resolution requires either several DOR tones at intermediate frequencies, or a ground receiver system with high phase-linearity. Also, as for spacecraft-spacecraft AVI.BI, the signals from the two

spacecraft must be at or near the same frequencies, unless the station receiver system digitizes the entire passband before downconversion to baseband.

As in the case of two orbiters, relative positioning information for a lander and rover may be obtained from an arc of SBI data without resolving the carrier cycle ambiguity. Only a carrier signal from each spacecraft is needed to enable this measurement. The performance for this case depends on the length of the data arc.

## **9. VLBI Compared to other Navigation Techniques**

Earth-based radio metric tracking is the primary source of navigational data during interplanetary cruise. Recent studies [e.g. Thurman and Eistefan 1993] predict that angular accuracy as good as 50 mrad can be inferred, in some cases, from long arcs of line-of-sight Doppler data. The advantages of using ADOR measurements are:

- ADOR provides a direct geometric measure of plane-of-sky position. Orbit solutions based on ADOR data show differing sensitivities to system errors, as compared to orbit solutions based on only line-of-sight measurements. Solutions which incorporate ADOR do not have singularities at low geocentric declinations or other adverse geometries.
- Comparable trajectory accuracy is obtained using either short arc (few days) or long arc (few months) solutions when ADOR data are used. Spacecraft state can be recovered more quickly following a maneuver.
- Navigation requirements can be satisfied by 1 hr of tracking time per week, thus reducing both the duration and number of weekly tracking passes.
- ADOR data may be acquired in a listen-only mode; an uplink is not required.
- ADOR data can provide improved angular accuracy.

## **10. Summary**

A ADOR measurement is generated by comparing, at two ground stations, the phases of two or more tones emitted by a spacecraft, and by measuring the difference in time of arrival, at the same two stations, of a broadband quasar signal.

It is preferable for DOR tones to be frequency coherent with the downlink carrier. This facilitates the detection of weak DOR tones by allowing the use of a phase model derived from the received carrier signal.

Signal detection requires a threshold of  $\frac{P_{\text{tone}}}{N_0} \geq 13 \text{ dB} \cdot \text{Hz}$  for a spacecraft tone alone as compared to a threshold of  $\frac{P_{\text{tone}}}{N_0} \geq 1 \text{ dB} \cdot \text{Hz}$  for a spacecraft tone which is a coherent submultiple of a spacecraft carrier signal ,

The ADOR measurement error is typically dominated by uncertainties due to quasar SNR, quasar position, instrumental phase ripple, and troposphere. Doubling the spanned bandwidth of the spacecraft DOR tones, while holding other parameters fixed, will halve the errors due to spacecraft SNR, quasar SNR, and instrumental phase ripple.

At S-band, one tone provides for ambiguity resolution and provides the widest bandwidth that fits within the allocation. At X-band, two tones are generally needed to provide for both ambiguity resolution and for high accuracy. At Ka-band, a wider spanned bandwidth is necessary to control the size of the error due to quasar SNR. Three tones are needed at Ka-band to provide for ambiguity resolution and to produce a sufficiently wide spanned bandwidth.

### **Acknowledgments**

The research described in this paper was performed at the Jet Propulsion Laboratory, California Institute of Technology, under contract with the National Aeronautics and Space Administration.

### **References**

- J. S. Border, W. M. Folkner, R. L. Kahn, and K. S. Zukor, "Precise Tracking of the Magellan and Pioneer Venus Orbiters by Same-Beam Interferometry, Part I: Data Accuracy Analysis," The Telecommunications and Data Acquisition Progress Report 42-110, Jet Propulsion Laboratory, California Institute of Technology, Pasadena, California, August, 1992, pp. 1-20,
- P. S. Callahan, "An Analysis of Viking S-X Doppler Measurements of Solar Wind Columnar Content Fluctuations," The Deep Space Network Progress Report 42-44, Jet Propulsion Laboratory, California Institute of Technology, Pasadena, California, April, 1978, pp. 75-81.
- C. D. Edwards, "Ionospheric Errors for Phobos AVIABI," JPL Internal Document IOM 335.1-91-21, Jet Propulsion Laboratory, California Institute of Technology, Pasadena, California, July 8, 1991.
- C. D. Edwards, Jr., W. M. Folkner, J. S. Border, and L. J. Wind, "Spacecraft-Spacecraft Very Long Baseline Interferometry for Planetary Approach Navigation," Spaceflight Mechanics 1991, Vol. 75, Advances in the Astronautical Sciences, Univelt, Inc., San Diego.
- W. M. Folkner and J. S. Border, "Orbiter-orbiter and Orbiter-lander Tracking Using Same-Beam Interferometry," The Telecommunications and Data Acquisition Progress Report 42-109, Jet Propulsion Laboratory, California Institute of Technology, Pasadena, California, May, 1992, pp. 74-86.

C. E. Hildebrand and T. P. Yunck, "Addendum to 'A Surprising Discovery in the Spectrum of the Voyager 2 X-band Signal'," JPL Internal Document IOM 335.4-98, Jet Propulsion Laboratory, California Institute of Technology, Pasadena, California, March 1, 1982.

R. 1). Kahn, W. M. Folkner, C. D. Edwards, and A. Vijayaraghavan, "Position Determination of a Lander and Rover at Mars With Earth-Based Differential Tracking," Jet Propulsion Laboratory TDA Progress Report 42-108, February, 1992, pp. 279-293.

K. M. Liewer, "DSN Very Long Baseline Interferometry System Mark IV-88," The Telecommunications and Data Acquisition Progress Report 42-93, Jet Propulsion Laboratory, California Institute of Technology, Pasadena, California, May, 1988, pp. 239-246.

J. B. Thomas, "An Error Analysis for Galileo Angular Position Measurements with the Block I ADOR System," JPL Internal Document EM 335-26, Jet Propulsion Laboratory, California Institute of Technology, Pasadena, California, November 11, 1981.

J. B. Thomas, "Interferometry Theory for the Block II Processor," JPL Publication 87-29, Jet Propulsion Laboratory, California Institute of Technology, Pasadena, California, October 15, 1987.

S. W. Thurman and J. A. Estefan, "Radio Doppler Navigation of Interplanetary Spacecraft Using Different Data Processing Modes," paper AAS-93-163, AAS/AIAA Spaceflight Mechanics Meeting, Pasadena, CA, February 22-24, 1993.